



HHS Public Access

Author manuscript

J Cardiovasc Electrophysiol. Author manuscript; available in PMC 2022 July 01.

Published in final edited form as:

J Cardiovasc Electrophysiol. 2021 July ; 32(7): 1857–1864. doi:10.1111/jce.15097.

Esophageal luminal temperature rise during atrial fibrillation ablation is associated with lower radiofrequency electrode distance and baseline impedance

Mirmilad Khoshknab, MD¹, Ling Kuo, MD^{1,2,3}, Tarek Zghaib, MD¹, Jeffrey Arkles, MD¹, Pasquale Santangeli, MD, PhD¹, Francis E. Marchlinski, MD¹, Yuchi Han, MD¹, Benoit Desjardins, MD, PhD⁴, Saman Nazarian, MD, PhD¹

¹Cardiovascular Medicine Division, University of Pennsylvania School of Medicine, Philadelphia, Pennsylvania, USA

²Division of Cardiology, Department of Internal Medicine, Heart Rhythm Center, Taipei Veterans General Hospital, Taipei, Taiwan

³Department of Medicine, National Yang-Ming University School of Medicine, Taipei, Taiwan

⁴Department of Radiology, University of Pennsylvania School of Medicine, Philadelphia, Pennsylvania, USA

Abstract

Introduction: Esophageal injury during atrial fibrillation (AF) ablation is a life-threatening complication. We sought to measure the association of esophageal temperature attenuation with radiofrequency (RF) electrode impedance, contact force, and distance from the esophagus.

Methods: The retrospective study cohort included 35 patients with mean age 64 ± 10 years, of whom 74.3% were male, and 40% had persistent AF. All patients had undergone preprocedural cardiac magnetic resonance (CMR) followed by AF ablation with luminal esophageal temperature monitoring. Lesion locations were co-registered with CMR image segmentations of left atrial and esophageal anatomy. Luminal esophageal temperature, time matched RF lesion data, and ablation distance from the nearest esophageal location were collected as panel data.

Results: Luminal esophageal temperature changes corresponding to 3667 distinct lesions, delivered with mean power 27.9 ± 5.5 W over a mean duration of 22.2 ± 10.5 s were analyzed. In multivariable analyses, clustered per patient, examining posterior wall lesions only, and adjusted for lesion power and duration as set by the operator, lesion distance from the esophagus ($-0.003^\circ\text{C}/\text{mm}$, $p < .001$), and baseline impedance ($-0.015^\circ\text{C}/\Omega$, $p < .001$) were associated with changes in luminal esophageal temperature.

Correspondence Saman Nazarian, MD, PhD, University of Pennsylvania Perelman School of Medicine. Spruce Street, Founders 9118, Philadelphia, PA 19104, USA., Saman.Nazarian@penmedicine.upenn.edu.

CONFLICT OF INTERESTS

Dr. Nazarian is a consultant for CardioSolv and Circle CVI; and principal investigator for research funding from Biosense Webster, ImriCor, Siemens, ADAS software and the US NIH. The University of Pennsylvania Conflict of Interest Committee manages all commercial arrangements. The other authors report no conflict of interests.

Conclusion: Esophageal luminal temperature rises are associated with shorter lesion distance from esophagus and lower baseline impedance during RF lesion delivery. When procedural strategy requires RF delivery near the esophagus, selection of sites with higher baseline impedance may improve safety.

Keywords

atrial fibrillation; catheter ablation; electrophysiology; impedance

1 | INTRODUCTION

Catheter ablation is routinely utilized for treatment of symptomatic atrial fibrillation (AF).¹⁻³ With the evolution of pulmonary vein isolation (PVI) to involve antral tissue,² and expansion of lesion sets to posterior wall targets,⁴ esophageal susceptibility to injury is increasingly relevant.^{1,2} Esophageal perforation is a serious complication of AF ablation with a reported incidence range from 0.02% to 0.2%.^{5,6} Atrio-esophageal fistula is the second most common cause of mortality after AF ablation, accounting for more than 16% of deaths. The diagnosis of esophageal perforation with and without atrial-esophageal fistula is associated with 79% and 13% mortality, respectively.⁵ To prevent esophageal injury, many strategies have been utilized including titration of lesion power/duration with monitoring of luminal esophageal temperature,⁷ intracardiac echocardiography for esophageal imaging during the procedure,⁸ mechanical deflection of the esophagus,⁹ esophageal cooling techniques,¹⁰ and/or esophageal insulation.¹¹ When performing the procedure under general anesthesia, esophageal luminal temperature monitoring during AF ablation is generally utilized in clinical practice.¹²⁻¹⁵ However, the specific variables that predict luminal temperature variations during AF ablation have not been objectively assessed. We sought to measure the association of esophageal temperature attenuation with radiofrequency (RF) electrode impedance, contact force, and distance from the esophagus.

2 | METHODS

2.1 | Study population

The source AF ablation cohort at the Hospital of the University of Pennsylvania was retrospectively queried to identify patients that underwent RF catheter ablation of AF and a preprocedural cardiac magnetic resonance (CMR) examination between January 2016 and January 2020. The study was approved by our institutional review committee, and all patients gave informed consent for the use of imaging and ablation data for medical research before the procedure. Patients with poor quality CMR due to motion or device artifact, without complete angiography and three-dimensional late gadolinium enhanced (LGE) images, without full procedural duration luminal temperature monitoring data, and/or electroanatomic map and lesion parameter data were excluded. The final study cohort consisted of 35 patients.

2.2 | Cardiac magnetic resonance

A 1.5 Tesla (Aera; Siemens) scanner was used to obtain CMR images, within 30 days of the procedure, with a cardiac-phased array receiver surface coil and electrocardiographic gating.

Gadoterate meglumine contrast (Dotarem; Guerbet LLC) at 0.2 mmol/kg was injected before magnetic resonance time-resolved angiography with interleaved stochastic trajectories imaging (TWIST) to define left atrial anatomy (field of view of 340–390 mm, echo time of 0.93–0.98 ms, repetition time of 2.6 ms, in-plane resolution of 1.22×1.22 mm, and slice thickness of 1.2 mm). LGE-CMR images were obtained using a 3D inversion recovery, 20–25 min after injection of contrast using a gradient-echo pulse sequence, with respiratory navigation and electrocardiographic gating (field of view of 3.5–3.9 cm, echo time of 1.3–1.6 ms, repetition time of 700–870 ms, inversion time of 310–350 ms, in-plane resolution of 1.37×1.37 mm, and slice thickness of 1.5 mm). The set-off time for the 3D LGE-CMR scan was modified to receive data during left atrial diastole with adjustment of the inversion time, based upon inversion time scout, to null normal myocardial signal.

2.3 | AF ablation

Heparin was administered intravenously to obtain an activated clotting time of more than 350 s before transseptal access. The transseptal sheaths were advanced to the superior vena cava over a long guidewire, and a flushed BRK transseptal needle was introduced into the Agilis/SL-1 sheaths. Then, the atrial septum was punctured using the BRK needle followed by fluoroscopic, hemodynamic pressure, and intracardiac echocardiography guided advancement of the dilator and sheath into the left atrium. Multipolar catheter mapping via the PentaRay (20 electrodes with 2–6–2 mm spacing; Biosense Webster) catheter and the Carto 3 (Biosense Webster) electroanatomic system was used to create three dimensional electrogram and anatomic maps. RF ablation was performed using a 3.5-mm open-irrigated Thermocool Smarttouch, or Thermocool Smarttouch SF (Biosense Webster), targeting the isolation of wide pulmonary vein antra together with ablation of spontaneous or inducible non-pulmonary vein triggers. Lesion power and duration varied per operator preference and was delivered at 25–50 W over 10–60 s anteriorly, and 20–50 W over 5–30 s posteriorly. Pulmonary vein entrance and exit was confirmed, and adenosine and/or isoproterenol were administered to survey acute reconnection with further ablation as necessary. Lesions delivered to the posterior wall were delivered with at least 1 cm distance between consecutive lesions to avoid temperature buildup with consecutive adjacent lesions. Temperature measurements were collected using a single sensor probe (Mon-a-Therm; Covidien-Medtronic). The probe was moved using fluoroscopy to match ablation catheter height while ablating on the posterior wall. Continuous (1 recording/min) luminal esophageal temperature monitoring data were collected.

2.4 | Electroanatomic map to image registration

Image analysis was performed retrospectively using ADAS software (Galgo). The left atrium and esophagus were manually contoured on axial 3D LGE images. Using this method, esophageal anatomy and position with respect to the left atrium and pulmonary veins was defined, as shown in Figure 1. The exact anatomy of the left atrium was then created by segmentation of the magnetic resonance angiogram. Left atrial volume was obtained from the 3D contours. Using left atrial surface alignment, the esophagus (from LGE) and left atrial anatomy (from magnetic resonance angiography) were registered. Electroanatomic map points were then imported into the ADAS software for surface alignment with left atrial and esophageal CMR (using pulmonary veins and the posterior

wall as landmarks). Distance between the esophagus and every ablation point was calculated by ADAS software. Lesions were identified as having been applied to the posterior wall if they were posterior to a line bisecting each pulmonary vein and the left atrium into anteroposterior halves. Each lesion end time was time matched to unique esophageal temperatures. Since the esophageal temperatures were recorded on a per minute frequency and given the expected 20–30 s lag between ablation lesion application and temperature changes, lesion end times between two discrete minutes were rounded up (i.e., lesion applied at 45:20 to 45:50, matched to temperature recording at minute 46:00).

2.5 | Statistical analysis

Continuous variables are summarized as mean \pm SD and categorical variables are summarized as numbers and percentages. Ablation parameter data for each individual lesion, distance from the esophagus, and corresponding esophageal temperatures were collated as panel data. To avoid Simpson's paradox and confounding related to interpatient differences, the association of temperature changes with ablation parameters and lesion distance from the esophagus was examined using generalized estimating equation linear regression models, clustered by patient and adjusted for lesion power and duration. $p < .05$ was considered statistically significant. Analyses were performed using STATA statistical software (version 15).

3 | RESULTS

3.1 | Baseline characteristics of patients

The final study cohort consisted of 35 patients with symptomatic AF. Baseline characteristics have been summarized in Table 1. The mean age was 64 ± 10 years, 74.3% were male, and 40% had persistent AF. Left Ventricular ejection fraction and diastolic diameter were $54.4 \pm .6\%$ and 56.4 ± 9.7 mm, respectively. Of all patients, 3 (8.6%) had history of coronary artery disease and 12 (34.3%) had previously diagnosed hypertension. Left atrial volume was associated with esophageal luminal temperature (regression coefficient $0.022^\circ\text{C}/\text{cm}^3$, $p = .025$). Other patient level factors including age, sex, AF persistence, and body mass index were unassociated with esophageal temperature changes.

3.2 | Ablation lesion parameters, distance from esophagus, and temperature changes

All patients underwent PVI and 12 (33%) had posterior wall isolation. In total, 3667 distinct lesions, corresponding parameters, and luminal esophageal temperatures were examined. Of all lesions, 2274 (62%) were on the posterior side of the pulmonary veins or the left atrium. The mean lesion parameters and esophageal temperatures during all lesions, posterior lesions and anterior lesions, as well as overall, between patient, and within patient SDs have been summarized in Table 2. Posterior wall lesions were on average applied with lower power, shorter duration, and lower contact force compared to those applied to the anterior wall. Contact of the esophagus and the posterior left atrium was closest in the lower half of the left atrium in a craniocaudal direction. The position of the esophagus in the upper half of the left atrium was closest to the left sided pulmonary veins in 12 (33%), the right sided pulmonary veins in 9 (25%), and in the middle of the left atrium in 15 (42%) patients. The position of the esophagus in the lower half of the left atrium was closest to the left sided

pulmonary veins in 5 (14%), the right sided pulmonary veins in 15 (42%), and in the middle of the left atrium in 16 (44%) patients.

Table 3 summarizes the univariable association of temperature as dependent variable with RF electrode contact force, distance from esophagus, and impedance as independent variables. On univariable analyses, all lesion parameters aside from force were negatively associated with temperature change. Each 1 mm additional lesion distance from the esophagus was associated with -0.006°C change in temperature. Each 1 Ω increased baseline impedance was associated with -0.017°C change in temperature. Each 1 Ω larger impedance drop was associated with -0.016°C change in temperature. In contrast, each gram increase in force was associated with 0.003°C change in temperature. When examining posterior wall lesions only, the direction of univariable associations was preserved in all cases; however, contact force was no longer associated with esophageal luminal temperature change. Univariable associations of interest are graphically summarized in Figure 2.

On multivariable analysis, summarized in Table 4, all parameters remained independently associated with esophageal luminal temperature change; however, the direction of association for impedance drop changed to positive. Each 1 mm additional lesion distance from the esophagus was associated with -0.004°C change in temperature. Each 1 Ω increased baseline impedance was associated with -0.017°C change in temperature. In contrast, each gram increase in contact force was associated with 0.002°C change in temperature. Each 1 Ω larger impedance drop was associated with 0.007°C change in temperature. When examining posterior wall lesions only, the direction of multivariable associations was preserved in all cases; however, contact force and impedance drop were no longer associated with esophageal luminal temperature change. Lesion distance from the esophagus ($-0.003^{\circ}\text{C}/\text{mm}$, $p < .001$), and baseline impedance ($-0.015^{\circ}\text{C}/\Omega$, $p < .001$) remained independently associated with changes in luminal esophageal temperature. Based upon the multivariable regression models, distance to closest esophageal border thresholds of 17, 16, and 15 mm correspond to 0.5°C , 1.0°C , and 1.5°C esophageal luminal temperature rises. Similarly, baseline impedance thresholds of 141, 137, and 134 Ω correspond to 0.5°C , 1.0°C , and 1.5°C esophageal luminal temperature rises.

4 | DISCUSSION

We aimed to define the association of RF electrode distance from the esophagus, contact force, and impedance with esophageal temperature changes during AF ablation. The major findings were that, after adjusting for lesion power and duration in multivariable models, esophageal luminal temperature increased (1) with decreased lesion distance from esophagus measured on preacquired CMR, and (2) with lower baseline impedance at the site of lesion delivery.

4.1 | Esophageal temperature, lesion parameters, and distance from esophagus

Continuous monitoring of esophageal luminal temperature during AF ablation is routinely utilized,^{12–15} and appears to be associated with reduced periesophageal nerve injury leading to gastric hypomotility, which is a practical proxy of esophageal compromise.¹⁶ In this study, the esophageal luminal temperature was used as a surrogate of esophageal muscular

heating abutting the epicardial left atrium. After adjusting for RF power and duration, parameters which were altered according to proximity to esophagus and observed temperature changes at adjacent sites, we found important associations between increased luminal esophageal temperature and baseline impedance as well as lower distance from esophagus.

The association of lower distance from the esophagus with higher temperature rises is expected given the higher propensity for conductive heating to affect nearby structures. The importance here, is that images acquired up to 30 days before the procedure, provide important and relevant anatomical information regarding esophageal location relative to the left atrium and pulmonary vein antra. Although data regarding esophageal stability overtime are conflicting,¹⁷⁻¹⁹ it is likely that any esophageal movement in the posterior left atrium region is minimal, related to peristalsis, and unlikely to constrain the utility of preacquired images. A prior study by Sarairah et al.²⁰ found that endoscopically detected esophageal thermal lesions were negatively associated with the shortest distance between the esophageal lumen and the atrial endocardium. In Sarairah et al.'s²⁰ study, the association between distance of esophageal lumen and atrial endocardium was made using the shortest distance for any lesion, rather than on a per lesion basis as performed in our study; nevertheless the result parallels our findings. This association has also been made using fluoroscopic measurements of intrapulmonary vein catheters to the temperature probe as a surrogate of the true distance between the left atrial endocardium and the esophagus.^{21,22}

The association of lower baseline impedance with higher esophageal luminal temperature rise is a novel finding, and is biologically plausible given that with lower baseline impedance, more current is delivered at a given power and more conductive heating can be expected.²³ Additionally, esophageal muscular tissue abutting the epicardial posterior left atrium may lead to greater conductivity between the local left atrial tissue and the grounding patch compared to left atrial regions abutting epicardial fat or vasculature. Importantly, if the association is due to greater current delivery with lower baseline impedance at a set power level,²⁴ it is likely that methodologies that estimate lesion size based upon power, without incorporating baseline impedance or current delivery, will under-estimate lesion size in regions with lower baseline impedance.^{25,26}

The association of higher impedance drop with higher temperature rise, did not reach statistical significance once the analysis was limited to posterior wall lesions. However, the association is expected because with greater heating, more ionic motion and ionic conductivity is anticipated, which translates to a larger drop in resistance to current flow.²⁷ Prior studies have shown an association between greater impedance drop and steam pops,²⁸ as well as lesion efficacy and durability.²⁹ It is important to note that the direction of association between the size of impedance drop and esophageal luminal temperature rise changed to fit clinical experience with ablation behavior upon addition of baseline impedance into the multivariable model. Therefore, it is the magnitude of impedance drop in relation to baseline impedance that deserves attention. As a direct surrogate of tissue heating, higher impedance drops, particularly in regions with low baseline impedance, should be avoided when lesions are delivered in close proximity to the esophagus.

4.2 | Clinical utility

Inadvertent thermal esophageal injury, as a result of conductive heating^{12,30–33} during AF ablation can result in esophageal erythema, ulceration, and subacute perforation and atrio-esophageal fistula formation. Although the incidence of atrio-esophageal fistula formation following AF ablation is low,³⁴ it is associated with an unacceptably high mortality rate approaching 80%.^{6,35} Therefore, any data that sheds light on factors affecting esophageal heating is valuable to inform the safest procedural strategy including ablation parameters. Based upon our findings, lesion distance from the esophagus should be maximized using preacquired or intraprocedural imaging. When procedural strategy requires RF delivery within 17 mm of the esophagus, sites with baseline impedance over 141 Ω may provide enhanced safety. As always, RF delivery should be ceased if a large impedance drop is noted.

4.3 | Limitations

This was a retrospective single center study with a relatively small sample size. However, many data points were analyzed, and the associations were statistically robust. The cohort was not consecutive as patients with missing CMR, esophageal temperature, electroanatomic map and lesion data, and those with suboptimal images were excluded. Data regarding RF lesions and temperature were retrospectively aligned using ablation and temperature time stamps and minor misalignments may exist. Lesion locations on electroanatomic maps and CMR were retrospectively registered and minor registration errors are possible. CMR was acquired up to 30 days before the procedure. However, the association between temperature and electrode distance from esophageal wall suggests that left atrial volume changes and esophageal motility do not constrain the utility of preacquired images. Optimal contact between the luminal temperature probe and esophageal wall is necessary for accurate monitoring of esophageal wall temperature and is impossible to ensure. Temperature was measured using a single thermistor probe. Although the probe was actively moved to match ablation catheter height while ablating on the posterior wall, the position may not have been optimal in some cases. Future studies using multi-sensor temperature probes and/or real-time CMR thermography may provide more accurate estimates of esophageal temperature and predictors of injury. Sequentially distant posterior wall lesions were performed to avoid progressive heating with adjacent lesions. However, summation of lesions overtime may have biased the associations under study. Due to operator awareness of temperature and lesion position and control of RF power and duration, we adjusted for but did not quantitate the latter variables' association with esophageal luminal temperature. Future studies with standardized variation of lesion power and duration are necessary to quantitate the association of power and RF duration with esophageal temperature.

5 | CONCLUSIONS

We report a close association between increased esophageal luminal temperature and decreased lesion distance from esophagus and lower baseline impedance before RF lesion delivery. Attention to these findings may improve the safety of AF ablation.

ACKNOWLEDGMENTS

Dr. Kuo is supported by Taipei Veterans General Hospital-National Yang-Ming University Excellent Physician Scientists Cultivation Program, No. 106-V-A-009. The study was also funded by a Biosense Webster Grant to Dr Nazarian and the Koegel Family EP Research Fund. Dr. Nazarian's research laboratory is supported by NIH grants R01HL116280 and R01HL142893, which indirectly supported this research. The contents do not necessarily represent the views of the National Institutes of Health.

Funding information

National Heart, Lung, and Blood Institute, Grant/Award Number: R01HL142893

DATA AVAILABILITY STATEMENT

The data that support the findings of this study are available from the corresponding author upon reasonable request.

REFERENCES

1. January CT, Wann LS, Calkins H, et al. AHA/ACC/HRS focused update of the 2014 AHA/ACC/HRS Guideline for the management of patients with atrial fibrillation: a report of the American College of Cardiology/American Heart Association Task Force on Clinical Practice Guidelines and the Heart Rhythm Society in Collaboration With the Society of Thoracic Surgeons. *Circulation*. 2019;2019(140):e125–e151.
2. Cappato R, Calkins H, Chen SA, et al. Updated worldwide survey on the methods, efficacy, and safety of catheter ablation for human atrial fibrillation. *Circ Arrhythm Electrophysiol*. 2010;3:32–38. [PubMed: 19995881]
3. Hindricks G, Potpara T, Dagres N, et al., ESC Scientific Document Group. 2020 ESC Guidelines for the diagnosis and management of atrial fibrillation developed in collaboration with the European Association of Cardio-Thoracic Surgery (EACTS). *Eur Heart J*. 2020;42(5):373–498.
4. Bai R, Di Biase L, Mohanty P, et al. Proven isolation of the pulmonary vein antrum with or without left atrial posterior wall isolation in patients with persistent atrial fibrillation. *Heart Rhythm*. 2016;13:132–140. [PubMed: 26277862]
5. Garg L, Garg J, Gupta N, et al. Gastrointestinal complications associated with catheter ablation for atrial fibrillation. *Int J Cardiol*. 2016;224: 424–430. [PubMed: 27690340]
6. Barbhuiya CR, Kumar S, Guo Y, et al. Global survey of esophageal injury in atrial fibrillation ablation: characteristics and outcomes of esophageal perforation and fistula. *JACC Clin Electrophysiol*. 2016;2:143–150. [PubMed: 29766863]
7. Leite LR, Santos SN, Maia H, et al. Luminal esophageal temperature monitoring with a deflectable esophageal temperature probe and intracardiac echocardiography may reduce esophageal injury during atrial fibrillation ablation procedures: results of a pilot study. *Circ Arrhythm Electrophysiol*. 2011;4:149–156. [PubMed: 21325208]
8. Bunch TJ, May HT, Crandall BG, et al. Intracardiac ultrasound for esophageal anatomic assessment and localization during left atrial ablation for atrial fibrillation. *J Cardiovasc Electrophysiol*. 2013;24: 33–39. [PubMed: 23067340]
9. Koruth JS, Reddy VY, Miller MA, et al. Mechanical esophageal displacement during catheter ablation for atrial fibrillation. *J Cardiovasc Electrophysiol*. 2012;23:147–154. [PubMed: 21914018]
10. Tsuchiya T, Ashikaga K, Nakagawa S, Hayashida K, Kugimiya H. Atrial fibrillation ablation with esophageal cooling with a cooled water-irrigated intraesophageal balloon: a pilot study. *J Cardiovasc Electrophysiol*. 2007;18:145–150. [PubMed: 17239114]
11. Nakahara S, Ramirez RJ, Buch E, et al. Intrapericardial balloon placement for prevention of collateral injury during catheter ablation of the left atrium in a porcine model. *Heart Rhythm*. 2010;7:81–87. [PubMed: 19914143]

12. Redfearn DP, Trim GM, Skanes AC, et al. Esophageal temperature monitoring during radiofrequency ablation of atrial fibrillation. *J Cardiovasc Electrophysiol.* 2005;16:589–593. [PubMed: 15946354]
13. Perzanowski C, Teplitsky L, Hranitzky PM, Bahnson TD. Real-time monitoring of luminal esophageal temperature during left atrial radiofrequency catheter ablation for atrial fibrillation: observations about esophageal heating during ablation at the pulmonary vein ostia and posterior left atrium. *J Cardiovasc Electrophysiol.* 2006;17: 166–170. [PubMed: 16533254]
14. Koranne K, Basu-Ray I, Parikh V, et al. Esophageal temperature monitoring during radiofrequency ablation of atrial fibrillation: a meta-analysis. *J Atr Fibrillation.* 2016;9:1452. [PubMed: 29250252]
15. Deneke T, Bunz K, Bastian A, et al. Utility of esophageal temperature monitoring during pulmonary vein isolation for atrial fibrillation using duty-cycled phased radiofrequency ablation. *J Cardiovasc Electrophysiol.* 2011;22:255–261. [PubMed: 20958829]
16. Kuwahara T, Takahashi A, Kobori A, et al. Safe and effective ablation of atrial fibrillation: importance of esophageal temperature monitoring to avoid periesophageal nerve injury as a complication of pulmonary vein isolation. *J Cardiovasc Electrophysiol.* 2009;20:1–6. [PubMed: 18775045]
17. Daoud EG, Hummel JD, Houmsse M, et al. Comparison of computed tomography imaging with intraprocedural contrast esophagram: implications for catheter ablation of atrial fibrillation. *Heart Rhythm.* 2008;5:975–980. [PubMed: 18598951]
18. Scazzuso FA, Rivera SH, Albina G, et al. Three-dimensional esophagus reconstruction and monitoring during ablation of atrial fibrillation: combination of two imaging techniques. *Int J Cardiol.* 2013;168:2364–2368. [PubMed: 23416012]
19. Starek Z, Lehar F, Jez J, et al. Esophageal positions relative to the left atrium; data from 293 patients before catheter ablation of atrial fibrillation. *Indian Heart J.* 2018;70:37–44. [PubMed: 29455785]
20. Sarairah SY, Woodbury B, Methachittiphan N, Tregoning DM, Sridhar AR, Akoum N. Esophageal thermal injury following cryoballoon ablation for atrial fibrillation. *JACC Clin Electrophysiol.* 2020; 6:262–268. [PubMed: 32192675]
21. Musat D, Aziz EF, Koneru J, et al. Computational method to predict esophageal temperature elevations during pulmonary vein isolation. *Pacing Clin Electrophysiol.* 2010;33:1239–1248. [PubMed: 20546158]
22. Barbhaiya CR, Kogan EV, Jankelson L, et al. Esophageal temperature dynamics during high-power short-duration posterior wall ablation. *Heart Rhythm.* 2020;17:721–727. [PubMed: 31978595]
23. Barkagan M, Rottmann M, Leshem E, Shen C, Buxton AE, Anter E. Effect of baseline impedance on ablation lesion dimensions: a multimodality concept validation from physics to clinical experience. *Circ Arrhythm Electrophysiol.* 2018;11:e006690. [PubMed: 30354405]
24. Bhaskaran A, Barry MA, Pouliopoulos J, et al. Circuit impedance could be a crucial factor influencing radiofrequency ablation efficacy and safety: a myocardial phantom study of the problem and its correction. *J Cardiovasc Electrophysiol.* 2016;27:351–357. [PubMed: 26648095]
25. Das M, Loveday JJ, Wynn GJ, et al. Ablation index, a novel marker of ablation lesion quality: prediction of pulmonary vein reconnection at repeat electrophysiology study and regional differences in target values. *Europace.* 2017;19:775–783. [PubMed: 27247002]
26. Kawaji T, Hojo S, Kushiyama A, et al. Limitations of lesion quality estimated by ablation index: an in vitro study. *J Cardiovasc Electrophysiol.* 2019;30:926–933. [PubMed: 30912209]
27. Inaba O, Nagata Y, Sekigawa M, et al. Impact of impedance decrease during radiofrequency current application for atrial fibrillation ablation on myocardial lesion and gap formation. *J Arrhythm.* 2018;34: 247–253. [PubMed: 29951139]
28. Seiler J, Roberts-Thomson KC, Raymond JM, Vest J, Delacretaz E, Stevenson WG. Steam pops during irrigated radiofrequency ablation: feasibility of impedance monitoring for prevention. *Heart Rhythm.* 2008;5:1411–1416. [PubMed: 18929327]
29. Yazaki K, Ejima K, Kanai M, et al. Impedance drop predicts acute electrical reconnection of the pulmonary vein-left atrium after pulmonary vein isolation using short-duration high-power exposure. *J Interv Card Electrophysiol.* 2020;59:575–584. [PubMed: 31902084]

30. Doll N, Borger MA, Fabricius A, et al. Esophageal perforation during left atrial radiofrequency ablation: is the risk too high? *J Thorac Cardiovasc Surg.* 2003;125:836–842. [PubMed: 12698146]
31. Aupperle H, Doll N, Walther T, et al. Ablation of atrial fibrillation and esophageal injury: effects of energy source and ablation technique. *J Thorac Cardiovasc Surg.* 2005;130:1549–1554. [PubMed: 16307997]
32. Cummings JE, Schweikert RA, Saliba WI, et al. Assessment of temperature, proximity, and course of the esophagus during radiofrequency ablation within the left atrium. *Circulation.* 2005;112:459–464. [PubMed: 16027254]
33. Zellerhoff S, Ullerich H, Lenze F, et al. Damage to the esophagus after atrial fibrillation ablation: just the tip of the iceberg? High prevalence of mediastinal changes diagnosed by endosonography. *Circ Arrhythm Electrophysiol.* 2010;3:155–159. [PubMed: 20194799]
34. Pappone C, Oral H, Santinelli V, et al. Atrio-esophageal fistula as a complication of percutaneous transcatheter ablation of atrial fibrillation. *Circulation.* 2004;109:2724–2726. [PubMed: 15159294]
35. Schmidt M, Nolker G, Marschang H, et al. Incidence of oesophageal wall injury post-pulmonary vein antrum isolation for treatment of patients with atrial fibrillation. *Europace.* 2008;10: 205–209. [PubMed: 18256125]

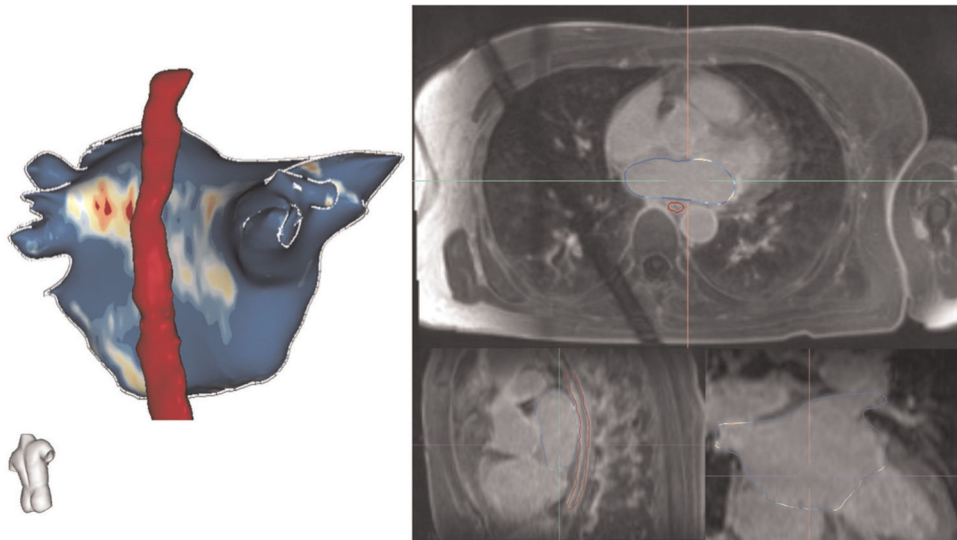


FIGURE 1. Process for segmentation of left atrial and esophageal anatomy. Using ADAS software (Galgo), the left atrium and esophagus were manually contoured on axial 3D LGE images. The exact anatomy of the left atrium was then created by segmentation of the magnetic resonance angiogram using intensity thresholding. Left atrial surface alignment was then utilized to register the esophagus (from LGE) and left atrial anatomy (from magnetic resonance angiography)

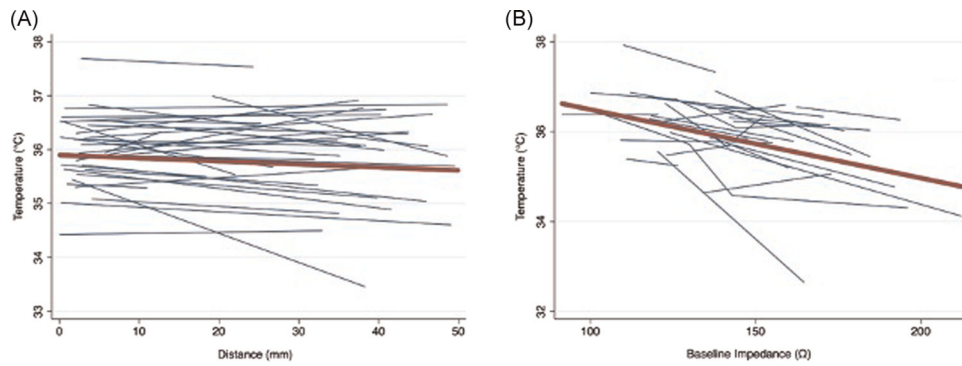


FIGURE 2.

Spaghetti plots of the univariable association of esophageal luminal temperature versus lesion distance and baseline impedance. The plots show a separate regression line (blue lines) for each patient representing the association between esophageal luminal temperature with (A) lesion distance and (B) baseline impedance. The line of best fit (red) represents the overall association as approximated by the univariable generalized estimating equations models in this study

TABLE 1

Baseline characteristics of study cohort

Variable	Mean ± SD or n (%)
Age, years	64 ± 10
LVEF, %	54.4 ± 7.6
Body mass index, kg/m ²	29.1 ± 4.9
Left atrial volume, cm ³	77.8 ± 14.4
Left ventricular diastolic diameter, mm	56.4 ± 9.7
Male	26 (74.3%)
Coronary artery disease	3 (8.6%)
Hypertension	12 (34.3%)
Persistent AF	14 (40%)

Author Manuscript

Author Manuscript

Author Manuscript

Author Manuscript

TABLE 2

Ablation lesion characteristics

Variable	Mean ± overall SD	Between patient SD	Within patient SD
Overall (<i>n</i> = 3667)			
Lesion duration, s	22.2 ± 10.5	5.5	8.9
Power, W	27.9 ± 5.5	3.3	4.8
Force, g	22.0 ± 9.6	4.4	8.8
Distance from esophagus, mm	22.3 ± 12.2	5.4	11.4
Baseline impedance, Ω	143.6 ± 20.2	17.4	10.1
Impedance drop, Ω	8.8 ± 5.1	2.4	4.7
Esophageal temperature, °C	35.8 ± 0.8	0.7	0.4
Posterior (<i>n</i> = 2274)			
Lesion duration, s	19.6 ± 8.6	4.1	7.4
Power, W	27.2 ± 5.5	3.4	4.9
Force, g	21.4 ± 9.5	4.9	8.3
Distance from esophagus, mm	17.8 ± 11.2	5.3	10.1
Baseline impedance, Ω	143.0 ± 20.3	17.5	9.9
Impedance drop, Ω	8.2 ± 5.0	2.3	4.6
Esophageal temperature, °C	35.8 ± 0.8	0.7	0.4
Anterior (<i>n</i> = 1393)			
Lesion duration, s	26.5 ± 11.9	7.4	9.3
Power, W	29.0 ± 5.4	3.9	4.2
Force, g	23.2 ± 9.7	6.3	8.9
Distance from esophagus, mm	29.6 ± 9.9	4.8	8.9
Baseline impedance, Ω	144.8 ± 19.9	18.1	9.7
Impedance drop, Ω	9.7 ± 5.2	2.6	4.5
Esophageal temperature, °C	35.7 ± 0.7	0.7	0.4

Note: g, gram; s, second; W, watts.

TABLE 3

Univariable association of temperature with radiofrequency electrode contact force, distance from esophagus, and impedance

	Univariable regression coefficient	<i>p</i>
Overall (<i>n</i> = 3667)		
Force, °C/g	0.003	<.001
Distance from esophagus, °C/mm	-0.006	<.001
Baseline impedance, °C/Ω	-0.017	<.001
Impedance drop, °C/Ω	-0.016	<.001
Posterior (<i>n</i> = 2274)		
Force, °C/g	0.002	.187
Distance from esophagus, °C/mm	-0.006	<.001
Baseline impedance, °C/Ω	-0.016	<.001
Impedance drop, °C/Ω	-0.013	<.001

Author Manuscript

Author Manuscript

Author Manuscript

Author Manuscript

TABLE 4

Multivariable association of temperature with radiofrequency electrode contact force, distance from esophagus, and impedance^a

	Multivariable regression coefficient	<i>p</i>
Overall (<i>n</i> = 3667)		
Force, °C/g	0.002	.046
Distance from esophagus, °C/mm	-0.004	<.001
Baseline impedance, °C/Ω	-0.017	<.001
Impedance drop, °C/Ω	0.007	.001
Posterior (<i>n</i> = 2274)		
Force, °C/g	0.001	.490
Distance from esophagus, °C/mm	-0.003	<.001
Baseline impedance, °C/Ω	-0.015	<.001
Impedance drop, °C/Ω	0.004	.119

^a Adjusted for lesion duration and power and left atrial volume.